# Supporting Information

# Fe and Cu co-doping induces abundant oxygen vacancies in $MnO_2$ for efficient ozone catalytic oxidation of toluene at room temperature

*Xinuo Cai*[a1], *Jiahong Liao*[a1], *Yushui Jiang*[d], *Yani Zhang*[a], *Lixia Qiu*[c], *Lecheng Lei*[a,b], *Chunlin Yu*[ab*], *Xingwang Zhang*[a]

[a] Key Laboratory of Biomass Chemical Engineering of Ministry of Education, College of Chemical and Biological Engineering, Zhejiang University, Hangzhou, 310027, China

[b] Institute of Zhejiang University-Quzhou, Quzhou, 324000, China

[c] Zhejiang Quzhou Jusu Chemical Co. Ltd., Quzhou, 324004, China

[d] Zhejiang Juhui New Material Co. Ltd., Quzhou, 324004, China

[1] These authors contributed equally to this work.

* Corresponding author

Email address: chunlinyu@zju.edu.cn

# 1. Experimental section

## 1.1 Details of XRD

Using X-ray diffraction (XRD) (XRD-6000, Shimadzu) within the scope from 5° to 80° to identify the series of catalysts crystal structure (scan step: 10°/min).

## 1.2 Details of SEM and HRTEM

Using Scanning electron microscopy (SEM) (SU8010, Hitachi, Ltd.) to observe the catalyst micro-morphology. Sample preparation: The catalyst powder was dispersed in ethanol and ultrasonicated for 1 h. An appropriate amount was taken from a capillary tube and dropped on a silicon wafer, which was then fixed on the sample stage with conductive adhesive. Gold spraying time: 120 s.

High-resolution transmission electron microscope (HRTEM) (JEM-F200, JEOL Ltd.) was used to further observe the lattice spacing. It is also equipped with an X-ray energy spectrometer to scan the surface of the material for elemental species and elemental distribution. Sampling preparation: a small amount of powder sample was dispersed in ethanol for 1 h, and then an appropriate amount of drops was pipetted onto the ultra-thin carbon film.

## 1.3 Details of XPS

X-ray photoelectron spectrometry (XPS) (K-Alpha, Thermo Scientific) equipped with Al target was used to analyze the elemental composition and chemical valence of sample surfaces. All the spectrums were calibrated by the C 1s peak at 284.6 eV.

## 1.4 Details of specific surface and porosity analysis

Using specific surface and porosity analyser (3Flex, Micromeritics) to analyze BET specific surface and pore size. Adsorption was carried out using 77 K liquid nitrogen followed by desorption for 8 h at 200℃. Specific surface area and pore structure information were calculated according to the BET and BJH methods, respectively.

## 1.5 Details of EPR

Electron paramagnetic resonance (EPR) (A300, Bruker) was used to anaylze the oxygen vacancy of catalysts. An appropriate amount of the powder sample was loaded into a 5 mm OD NMR tube with a height of about 4 cm. Test conditions: microwave power 19.12 mW, swept field range 3200-6000 G.

### 1.6 Details of $H_2$-TPR

Low temperature reducibility and oxygen mobility of catalysts were tested by temperature programmed chemisorption analyzer（AutoChem II 2920，Micromeritics）. Following pretreatment, the sample was loaded into the reactor, purged with argon for 30 min to eliminate residual air and moisture, then subjected to temperature-programmed heating (10°C/min, 25-800°C) under hydrogen flow. Hydrogen consumption was continuously monitored via a thermal conductivity detector (TCD), with the corresponding H2 concentration profile recorded.

### 1.7 Details of ICP

Inductively Coupled Plasma-Optical Emission Spectrometer (ICP-OES) (Optima 8300, PerkinElmer) was used to analyze the bulk doping concentration. The instrument parameters were as follows: RF Power 1150 W, Plsama flow 0.5 L/min, Auxiliary flow 0.5 L/min, Nebulizer flow 12.5 L/min, Sample uptake delay 30 s.

### 1.8 Details of electrochemical measurements

Cyclic voltammetry experiments of the catalysts were carried out on a standard three-electrode system of a Bio-Logic VSP constant potential apparatus with an electrolyte of 0.5 M $H_2SO_4$ solution saturated with oxygen. The prepared catalyst was coated on carbon paper (effective area of 1 $cm^2$) as the working electrode, and $Hg/Hg_2SO_4$ (containing saturated $K_2SO_4$ solution) and platinum column electrodes were used as the reference and counter electrodes, respectively. The scanning rate was 20 mV $s^{-1}$ and the voltage range was 0.4 V~1.0 V.

### 1.9 Details of DRIFTs

The degradation of toluene by $MnO_2$ catalytic ozonation was examined in the range of 500-4000 $cm^{-1}$ using in situ DRIFTs (Thermo Scientific). In situ DRIFTs spectra were performed on a Nicolet 6700 equipped with a liquid $N_2$-cooled mercury cadmium telluride (MCT) detector with a resolution of 4 $cm^{-1}$. The samples were pretreated with a stream of $N_2$ at 150 °C for 1 h to remove water and other contaminants adsorbed on the surface. Background spectra of the catalyst were collected after the reaction cell was cooled to room temperature. A gas mixture (25 °C, 100 ppm toluene

+ 1000 ppm ozone + dry air) was then introduced continuously into the in-situ diffuse reflectance cell and reacted for 120 min.

## 2. Results and discussion

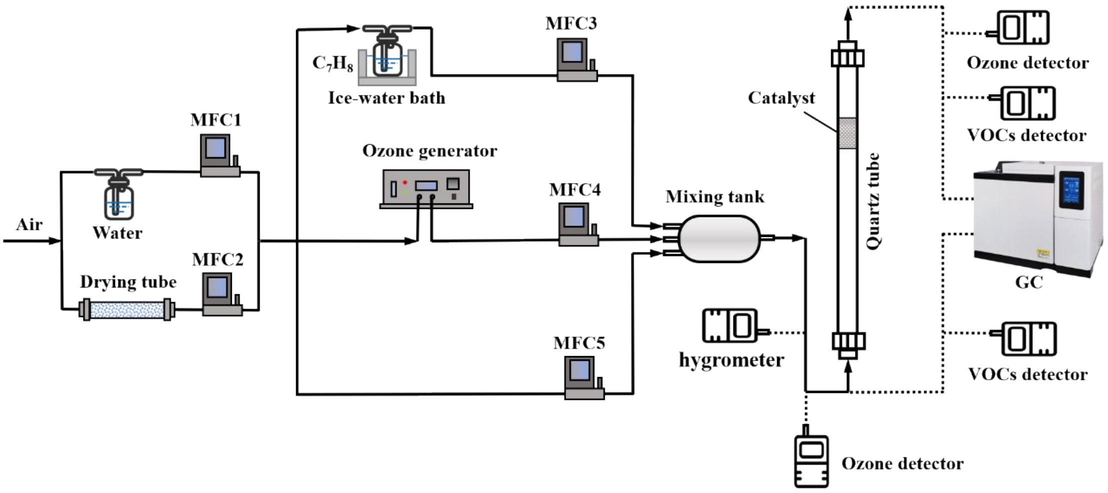

Figure. S1. Schematic diagram of the catalytic ozonation toluene performance assessment device.

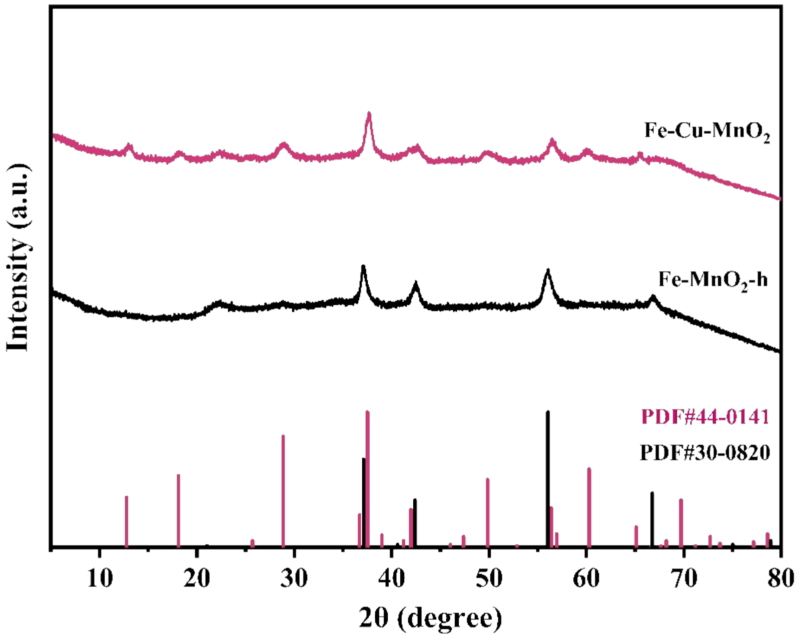

Fig. S2. XRD patterns of Fe-Cu-MnO$_2$ and Fe-MnO$_2$-h (for Fe-MnO$_2$-h, the designed atomic ratio of Fe/Mn was 0.3).

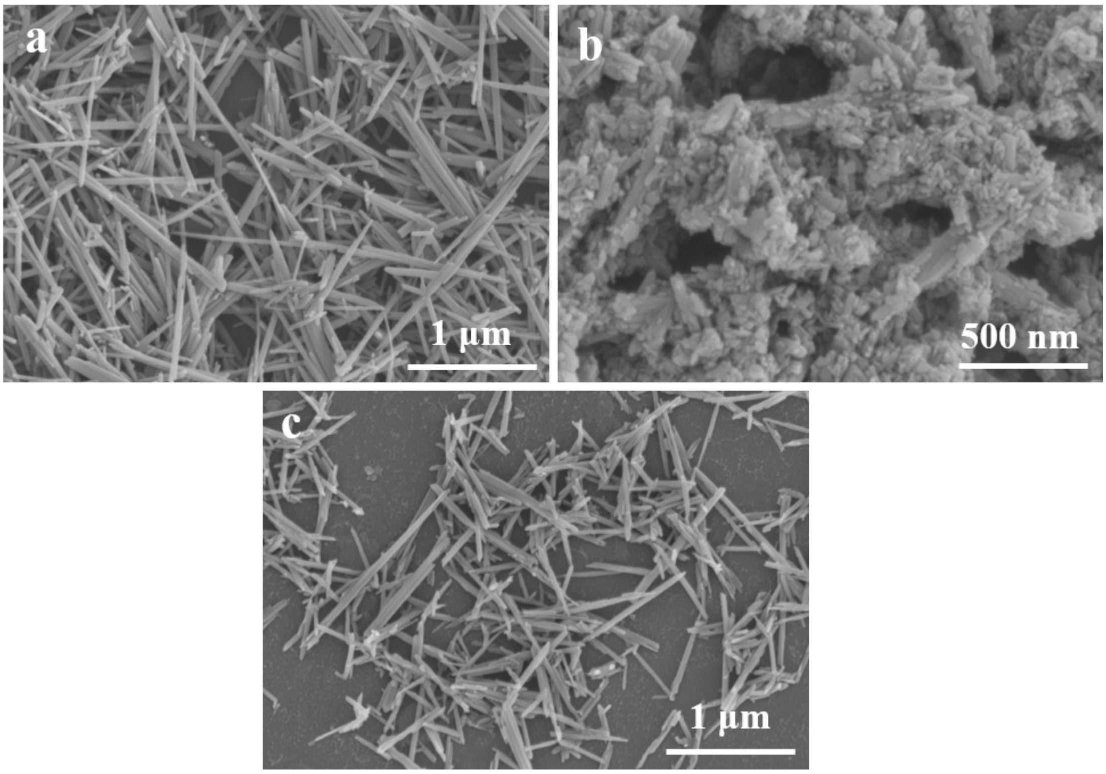

Fig. S3. (a) SEM image of MnO$_2$; (b) SEM image of Fe-MnO$_2$; (c) SEM image of Cu-MnO$_2$.

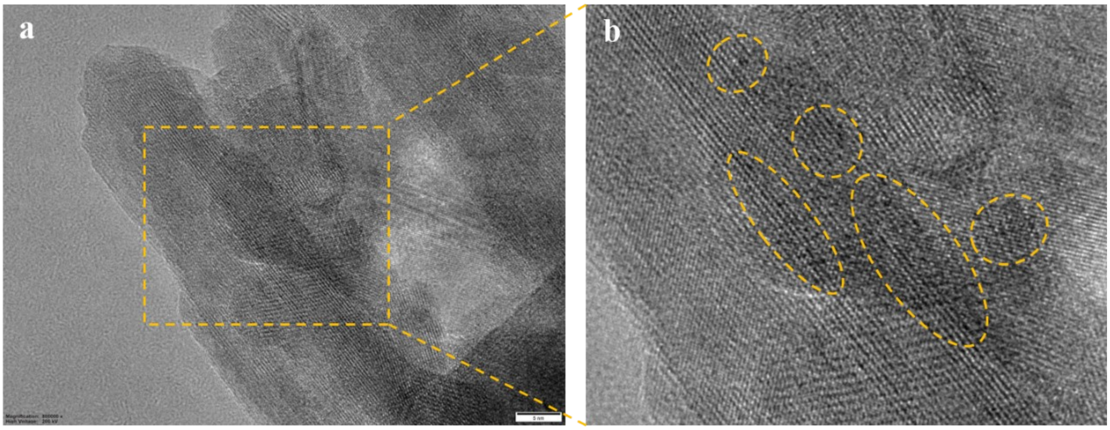

Fig. S4. TEM image of catalyst Fe-Cu-$MnO_2$ (orange dashed circles indicate oxygen vacancies).

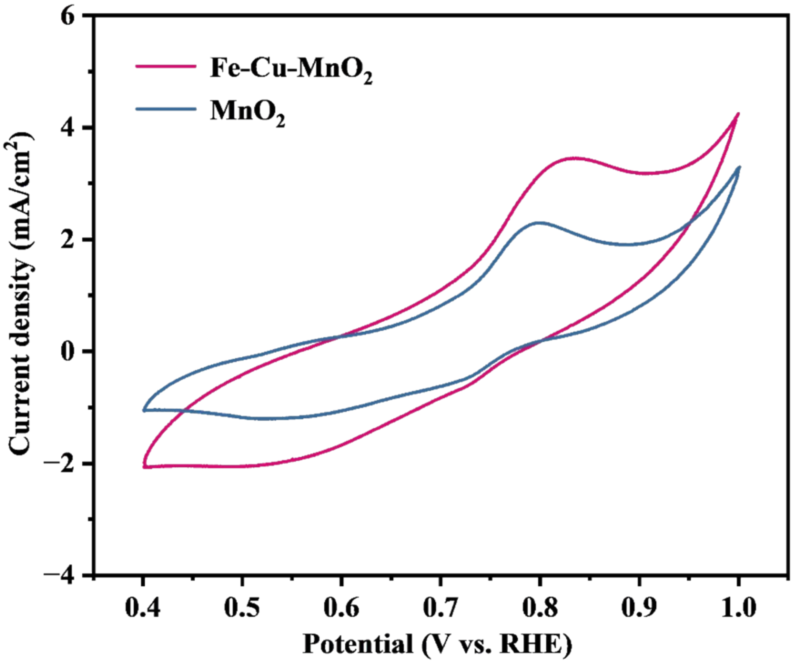

Fig. S5. Cyclic voltammetry (CV) curves of catalysts Fe-Cu-$MnO_2$ and $MnO_2$.

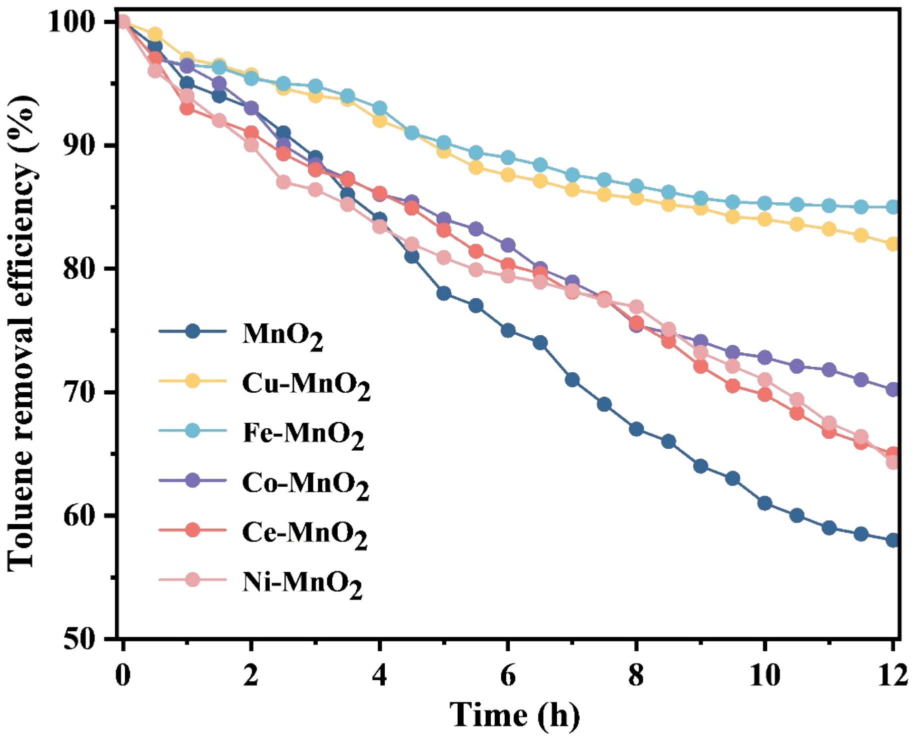

Fig. S6. Efficiency of $MnO_2$ catalytic ozonation of toluene with different cation doping (Fe, Cu, Co, Ce, Ni). (All cation additions were 0.75 mmol; reaction conditions were: inlet toluene concentration 100 ppm, inlet ozone concentration 1000 ppm, catalyst mass 50 mg, WHSV = 120,000 ml $g_{cat}^{-1}$ $h^{-1}$, humidity < 5% RH)

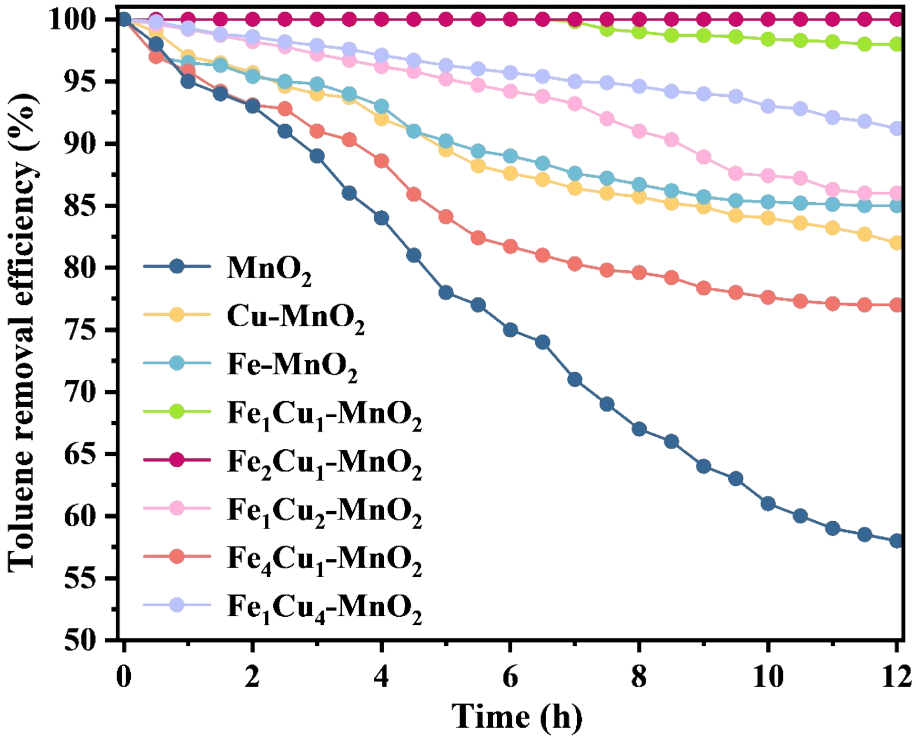

Fig. S7. Efficiency of catalytic ozonation of toluene by $MnO_2$ with different FeCu doping ratios. ($Fe_xCu_y$-$MnO_2$ means the designed atomic ratio of Fe/Cu was x/y, the sum of molar amounts of Fe and Cu was 0.75 mmol; reaction conditions were: inlet toluene concentration 100 ppm, inlet ozone concentration 1000 ppm, catalyst mass 50 mg, WHSV = 120,000 ml $g_{cat}^{-1}$ $h^{-1}$, humidity < 5% RH)

Table S1. Fe/Mn atomic ratio and Cu/Mn atomic ratio of different catalysts analyzed by ICP-OES and XPS.

| Catalysts | ICP-OES analysis | | XPS analysis | |
|---|---|---|---|---|
| | Fe/Mn (%) | Cu/Mn (%) | Fe/Mn (%) | Cu/Mn (%) |
| Fe-Cu-MnO$_2$ | 9.5 | 4.6 | 10.3 | 4.9 |
| Fe-MnO$_2$ | 14.3 | - | 14.7 | - |
| Cu-MnO$_2$ | - | 11.4 | - | 13.6 |

Table S2. Comparison of degradation efficiency and mineralization ratio of MnO$_x$

| catalysts | reaction temperature(°C) | WHSV | O$_3$:toluene (ppm:ppm) | degradation efficiency | mineralization ratio | Ref. |
|---|---|---|---|---|---|---|
| Fe-Cu-MnO$_2$ | 25 | 120000 ml❿g$^{-1}$❿h$^{-1}$ | 1000:100 | 100% | 81.2% | This work |
| Cu-Mn/DY | 30 | 170000 h$^{-1}$ | 3000:200 | 95% | 80% | 1 |
| Pt/FeO$_x$-180 | 50 | 90000 ml❿g$^{-1}$❿h$^{-1}$ | 2000:270 | 100% | --- | 2 |
| Cu$_{0.2}$MnO$_x$ | 100 | --- | 2100:160 | 91.2% | 83% | 3 |
| α-MnO$_2$ | room temperature | 30000 h$^{-1}$ | 90:30 | 51.7% | 7.5% | 4 |
| H-MA | 25 | 60000 ml❿g$^{-1}$❿h$^{-1}$ | 180:20 | 100% | 82.3% | 5 |
| α-MnO$_2$/Z-S2 | 30 | 32000 h$^{-1}$ | 45:5 | 87% | 94% | 6 |
| RuMnZ | room | 4200 h$^{-1}$ | 1000:100 | 36% | 61% | 7 |

temperature

# Reference

1. Q. Shao, S. Wei, X. Hu, H. Dong, T. Wen, L. Gao and C. Long, Tuning the Micro-coordination Environment of Al in Dealumination Y Zeolite to Enhance Electron Transfer at the Cu-Mn Oxides Interface for Highly Efficient Catalytic Ozonation of Toluene at Low Temperatures, *Environmental Science & Technology*, 2022, 56, 15449-15459.
2. R. Liu, S. Liu, H. Ding, D. Zhao, J. Fu, Y. Zhang, W. Huo and G. K. Li, Unveiling the Role of Atomically Dispersed Active Sites over Amorphous Iron Oxide Supported Pt Catalysts for Complete Catalytic Ozonation of Toluene at Low Temperature, *Industrial & Engineering Chemistry Research*, 2021, 60, 3881-3892.
3. Z. Ye, G. Wang, J.-m. Giraudon, A. Nikiforov, J. Chen, L. Zhao, X. Zhang and J. Wang, Investigation of Cu-Mn catalytic ozonation of toluene: Crystal phase, intermediates and mechanism, *Journal of Hazardous Materials*, 2022, 424.
4. R. Yang, Z. Guo, L. Cai, R. Zhu, Y. Fan, Y. Zhang, P. Han, W. Zhang, X. Zhu, Q. Zhao, Z. Zhu, C. K. Chan and Z. Zeng, Investigation into the Phase-Activity Relationship of $MnO_2$ Nanomaterials toward Ozone-Assisted Catalytic Oxidation of Toluene, *Small*, 2021, 17.
5. B. Zhang, Y. Shen, B. Liu, J. Ji, W. Dai, P. Huang, D. Zhang, G. Li, R. Xie and H. Huang, Boosting Ozone Catalytic Oxidation of Toluene at Room Temperature by Using Hydroxyl-Mediated $MnO_x/Al_2O_3$ Catalysts, *Environmental Science & Technology*, 2023, 57, 7041-7050.
6. W. Hong, Y. Liu, T. Zhu, H. Wang, Y. Sun, F. Shen and X. Li, Promoting the Catalytic Ozonation of Toluene by Introducing $SO_4^{2-}$ into the $\alpha$-$MnO_2$/ZSM-5 Catalyst to Tune Both Oxygen Vacancies and Acid Sites, *Environmental Science & Technology*, 2022, 56, 15695-15704.
7. J. Kim, J. E. Lee, H. W. Lee, J.-K. Jeon, J. Song, S.-C. Jung, Y. F. Tsang and Y.-K. Park, Catalytic ozonation of toluene using Mn-M bimetallic HZSM-5 (M: Fe, Cu, Ru, Ag) catalysts at room temperature, *Journal of Hazardous Materials*, 2020, 397.